

INTERACTION OF FEMTOSECOND LASER BEAM WITH ATMOSPHERIC LOW
TEMPERATURE PLASMAS AND ELECTRIC FIELDS

by

Kirtan Maheshbhai Davda

A thesis submitted to the faculty of
The University of North Carolina at Charlotte
in partial fulfilment of the requirements
for the degree of Master of Science in
Applied Energy and Electromechanical Systems

Charlotte

2017

Approved by:

Dr. Maciej Noras

Dr. Tsing-Hua Her

Dr. Wesley Williams

© 2017
Kirtan Maheshbhai Davda
ALL RIGHTS RESERVED

ABSTRACT

KIRTAN MAHESHBHAI DAVDA. Interaction of femtosecond laser beam with atmospheric low temperature plasmas and electric fields. (Under the direction of DR. MACIEJ NORAS)

In this work, the influence of electric fields and atmospheric plasma on behavior of an ultrafast femtosecond laser beam is being studied. A femtosecond laser pulse has an ability to self-focus in air and produce confined narrow channels of high energy density plasma, called filaments, which propagate over long distances. This technique has been employed in the remote initiation of electric discharges and has a potential to serve in lightning control, rain making, remote measurement of the electric field, microwave guidance and remote sensing of chemicals. Filamentation process requires significant amount of energy ($> \text{GW}$), and the lasers used for that purpose are large and not easy to deploy and use. In this research, a possibility of using external high electric fields and low-temperature plasmas is explored to augment the laser beam operation, with the goal of lowering the power requirement on the laser. These external fields and plasmas are intended to act as stimuli to achieve filamentation of ultrashort laser pulses at a lower energy of the laser beam. Ultimately this approach may lead to reduction of the size, weight, and power consumption of the laser system.

DEDICATION

This work is dedicated to my parents, Mahesh Davda and Aruna Davda, for supporting and encouraging me throughout my life, my sister and brother-in-law, Swati Panchal, and Bimal Panchal for always being available to help every time help is needed.

ACKNOWLEDGMENTS

First of all, I would like to thank Bhagwan Swaminarayan, Pramukh Swami Maharaj, and Mahant Swami Maharaj, for their grace with which I could achieve such knowledge and wisdom in my life.

I would like to sincerely thank my advisor, Dr. Maciej Noras, without whose expertise, guidance, and encouragement, this thesis could not have been possible. Dr. Noras has been so much more to me than just an advisor. His continuous support and help have taken this research to the next level. I would also like to thank my other advisor, Dr. Wesley Williams, whose continuous support, and proper directions have led me to learn many things throughout my thesis. I would also like to thank my committee member Dr. Tsing-Hua Her, whose expertise on laser and availability made this research an empirical one. I truly thank him for providing the laser equipment to help me go ahead with the thesis. I would also like to thank Dr. Barry Sherlock for his up to date check on my thesis and reminding me about the important dates throughout the semester.

I would like to thank Dr. Her's students, Mark Green, and Larkin Hipp whose support and expertise on setting up the laser system have helped me go ahead with my research. I would also like to thank Mr. Parks Davidson and Mr. Wesley Maxwell, for manufacturing the electrodes and the wooden stands for this research.

Finally, I would like to thank my parents, Mahesh Davda and Aruna Davda, for their continuous faith in me and encouraging me to do the right thing.

TABLE OF CONTENTS

LIST OF TABLES	ix
LIST OF FIGURES	x
UNITS.....	xii
CHAPTER 1: INTRODUCTION	1
1.1. An overview of previous work.....	2
1.2. Scope of the thesis.....	3
1.3. Outline of the thesis.....	4
1.4. The role of the author	5
CHAPTER 2: FILAMENTATION.....	6
2.1. Introduction	6
2.2. Properties of ultrashort laser pulse	7
2.2.1. Diffraction	8
2.2.2. Space-time defocusing	8
2.2.3. Self-focusing	9
2.2.4. Plasma defocusing.....	9
2.2.5. Refocusing cycles.....	10
2.2.6. Filaments in condensed media	11
2.3. Energy dynamics of the filament.....	12

2.4. Applications.....	13
2.4.1. LIDAR.....	13
2.4.2. Laser propulsion.....	14
2.4.3. Atmospheric Applications.....	15
2.4.4. Lightning Control.....	15
2.4.5. Laser Induced Breakdown Spectroscopy (LIBS).....	17
CHAPTER 3: LASER-ELECTRICAL FIELD INTERACTION	18
3.1. Introduction	18
3.2. Electric field	18
CHAPTER 4: LASER POWER MEASUREMENT	23
4.1. Introduction	23
4.2. Experiment Setup	23
4.2.1. Parallel plate electrode (T1).....	26
4.2.2. ‘V’ shaped electrode (T2)	28
4.2.3. Needle electrodes (T3)	29
4.2.4. Double helix shaped electrode (T4)	31
4.3. Results	34
4.3.1. Parallel plate electrode (T1).....	35
4.3.2. ‘V’ shaped electrode (T2)	37
4.3.3. Parallel plate electrode separated spatially (T3)	39

4.3.4. Double helix shaped electrode (T4)	41
CHAPTER 5: PROBABLE CONCLUSION AND DISCUSSIONS	43
5.1. Summary of the thesis	45
5.2. Future work.....	45
REFERENCES	46
APPENDIX I: List of refractive indices	51
APPENDIX II: Working of a gas laser.....	52
APPENDIX III: Ionization process	53

LIST OF TABLES

Table 1:	Comparing the electric field values of the laser system and externally applied electric field	21
Table 2:	Experimental result for T1 electrode DC supply	35
Table 3:	Experimental result for T1 electrode AC supply	36
Table 4:	Experimental result for T2 electrode DC supply	37
Table 5:	Experimental result for T2 electrode AC supply	38
Table 6:	Experimental result for T3 electrode DC supply	39
Table 7:	Experimental result for T3 electrode AC supply	40
Table 8:	Experimental result for T4 electrode DC supply	41
Table 9:	Experimental result for T4 electrode AC supply	42
Table 10:	List of refractive indices for common media	51

LIST OF FIGURES

Fig. 1.	Image of a filament	06
Fig. 2. a.	Self-focusing of a beam due to optical Kerr effect	09
Fig. 2. b.	Defocusing of the laser beam due to the presence of the plasma	09
Fig. 3.	Schematic representation of the refocusing cycles	10
Fig. 4.	Two regions of a filament	12
Fig. 5.	Schematic diagram of a white-light LIDAR	13
Fig. 6.	Laser control of high-voltage plasma discharge	16
Fig. 7.	Laser setup at Grigg 108. This setup shows the reflective mirrors from which the laser is shun towards the electrode setup	24
Fig. 8.	Schematic diagram of the laser setup in the Grigg Hall with the electrode in the path of the laser	25
Fig. 9.	Schematic diagram of the electric field through T1	27
Fig. 10.	Parallel plate electrode (T1)	27
Fig. 11.	Schematic of T1 electrode and the path of laser during the experiment.	28
Fig. 12.	T2 electrode geometry	28
Fig. 13.	T2 electrode connection and path of the laser	29
Fig. 14.	‘V’ shaped electrode system	29
Fig. 15.	Schematic diagram of T3 electrode and the path of laser	30
Fig. 16.	T3 electrode and the virtual path of the laser	31
Fig. 17.	Double helix electrode (T4)	32
Fig. 18.	Inside geometry of T4 electrode.	33

Fig. 19.	Inside geometry of T4 electrode with laser beam path	33
Fig. 20.	Influence of DC Electric field on T1 electrode system	35
Fig. 21.	Influence of AC Electric field on T1 electrode system	36
Fig. 22.	Influence of DC Electric field on T2 electrode system	37
Fig. 23.	Influence of AC Electric field on T2 electrode system	38
Fig. 24.	Influence of DC Electric field on T3 electrode system	39
Fig. 25.	Influence of AC Electric field on T3 electrode system	40
Fig. 26.	Influence of DC Electric field on T4 electrode system	41
Fig. 27.	Influence of AC Electric field on T4 electrode system	42

UNITS

V	Volt
kV	Kilo-Volt
W	Watt
mW	Milli-Watt
MW	Mega-Watt
GW	Giga-Watt
A	Ampere
mA	Milli-Ampere
m	meter
μm	Micro-meter
cm	Centi-meter
V/m	Volt per meter
kV/m	Kilo-Volt per meter
F/m	Faraday per meter
m/sec	Meters per second

CHAPTER 1: INTRODUCTION

It comes under general conscience that most of the matter in the world exists in three different states: solid, liquid, and gaseous. There is, in fact, a fourth state of matter that exists throughout the universe: plasma. Plasma is generally considered to be a charged gas with strong electrostatic force between the ions in it. It is the most common state of matter in the universe.

The noble gases are generally the medium to be ionized with electricity to create the plasma state. This process is well documented in the nuclear fusion reactors. Naturally occurring plasma can be especially seen in stars (for example sun). Seeing how powerful and dense the fourth state of matter can be, it is astonishing that the laser can produce it too. Although under special conditions, it is remarkable that lasers depict such phenomenon and produces plasma.

This process of producing plasma via laser under special condition is termed as filamentation. Since laser light and externally generated electric field have similar nature and both are capable of producing plasma, it might be possible for both to interact with each other. The research in this thesis is carried out in search of the above-mentioned possibility.

1.1. An overview of previous work

Extensive research has been conducted and numerous books and articles have been written describing laser filamentation phenomena. In 1960s researchers, could predict that an intense laser beam is capable of self-focusing and producing narrow plasma channels propagating along the beam's direction [1]. The experimental confirmation of creation of such filaments in various types of solids and liquid media was provided soon thereafter by many scientists (e.g. [2-5]). One of the important findings was that to observe plasma filaments, the power of the laser had to exceed certain threshold value. In solids and in liquid media this critical power is within a couple of MW, and in gases it is in a range of GW [6]. To pack more energy into the laser beam, while avoiding laser induced breakdown, a natural tendency was to use shorter pulses.

It was not until 1990s when technology developments permitted transition from nanosecond and picosecond pulses to the femtosecond scale, and the filamentation effect was for the first time recorded in gaseous media [7]. Very quickly the potential use of filamentation in guiding of electrical discharges and even in triggering of lightnings was proposed [8,9], followed by remote LIDAR and LIDAR-based sensing applications (e.g. [10-13]). These detection systems are known as remote filament-induced breakdown spectroscopy (R-FIBS), and start competing with traditional laser induced breakdown spectroscopy (LIBS) devices.

The main advantage over LIBS is that they do not require complex optical focusing systems and are not affected by fluctuation of atmospheric properties [14]. The drawbacks are high cost, size, and complexity, as they are still considered more feasible for laboratories rather than field deployment. For example, Teramobile, used frequently as the

prime example of a mobile terawatt laser filamentation system, is housed in a standard ISO 20 ft. cargo container (5.70 m x 2.15 m x 2.20 m), weights 10 tons (with all the associated control and analytics equipment), and its power consumption during operation is 30 kW [15].

More research is needed on making such systems more robust, compact, lighter and to reduce their power consumption. This thesis is written to set a framework for investigations that should help to achieve that goal.

1.2. Scope of the thesis

The process of femtosecond filamentation occupies a large room for housing the laser system and requires a lot of energy (GW) to initiate the process of filamentation. One of the ideas on lowering the size of the laser system is to enhance the laser beam power by means other than the power of the laser itself. This idea can be implemented using the external electric fields and plasmas created by the fields. This thesis discusses the measurement of power of the femtosecond laser beam after its interaction with low temperature plasmas and electric field. A new approach to a research topic is developed and discussed in this thesis; the interaction of ultra-fast femtosecond laser with externally generated electric fields and plasmas. This research topic has not yet been discussed in the physics community and this thesis tries to address the research question.

In the thesis, the interaction of femtosecond laser beam is studied with low temperature plasmas and strong electric field. This interaction is investigated by changes in power of the laser beam. The reason of choosing these parameters to interact with the

laser is a possible correlation of ultrafast laser with electric field and low temperature plasma.

It is known that the femtosecond laser has the capability to produce plasma due to the process of filamentation, but the effect of externally produced plasma on femtosecond laser is not yet known and studying the laser interaction with external plasma and electric field can lead to better understanding of the topic and may lead to efficient laser systems with more capable applications.

1.3. Outline of the thesis

The thesis is divided into chapters as follows:

Chapter 2 discusses the theories behind the self-focusing of the laser beam and its applications.

Chapter 3 discusses briefly the topic of electric field and low temperature plasma and its relationship with laser beam and how they can affect the laser beam. This chapter mainly reviews the “non-laser” part of the thesis.

Chapter 4 details the experimental setup and the results from the interaction of the femtosecond laser with low temperature plasma and electric field through four different electrode geometries.

Chapter 5 analyzes the observations made from Chapter 4 and summarizes the effect of four different electrode geometries with low temperature plasma and strong electric field on femtosecond laser beam. It also discusses possible future research directions.

1.4. The role of the author

The results presented in Chapter 4 and Chapter 5 were part of a single experiment carried out on the Tsunami and RegA femtosecond laser beam. This was carried out with the assistance of Ms. Bhavana Sahiti, Mr. Larkin Hipp and Dr. Maciej Noras. The author was involved in data acquisition, generation of high voltage plasma and setting up the electrodes.

The spatial, temporal and frequency dependent measurement were recorded in the laser facility in Grigg 108. The author was fully responsible and involved in the planning and setting up the electrode setup and manufacturing the electrodes. The laser alignment and setting up of the laser was done by Mr. Larking Hipp and the electrodes were made with the assistance of Mr. Luis Benitez-Peralta and Mr. Alzarrio Rolle.

The results and the probable conclusions presented on the thesis are concluded after consulting Dr. Tsing-Hua Her and Dr. Maciej Noras. The author is solely responsible for the experiments carried out and the analysis of the results.

CHAPTER 2: FILAMENTATION

2.1. Introduction

The phenomenon in which laser beam forms narrow channel by reaching high intensities to ionize its medium of propagation to create plasma is called filamentation. In other words, the process of creating plasma in the laser is called filamentation. The plasma thus created is called a filament and the process by which it is created is called filamentation [16].

Once the power of the laser exceeds its critical power, P_{cr} , the laser is intensified enough to converge and form narrow channels and tends to form a filament/plasma. This part of the process occurs due to optical Kerr effect, where there is change in refractive index of a material due to applied electric field. Once the plasma/filament is formed, due to diffraction, plasma defocusing and self-focusing, the laser tends to defocus locally. Since the laser tends to defocus, the energy of the laser diminishes, thus gradually weakening and eventually terminating the filament [16].

The laser filament can be as long as few several meters to a couple of meters when the filamentation process is applied at a longer distance of few kilometers in air [16]. A filament has an energetic structure with an intense core that keeps a narrow beam size over propagating over long distances without any external mechanisms. The intensity of the plasma is sufficient to ionize the molecules/atoms of the medium of propagation [17].

From the time laser was invented in the late 1950s, the research on the laser and its various properties has been studied continuously [16]. It was not until 1962, G. A. Askar'yan theorized the 'self-focusing' of the laser beam [5].

The technological advancement of laser system in late 20th century, made the high-power laser readily accessible and the phenomenon that was only noticed in dense media is now easily observed in gaseous media. An example of it being self-focusing and filamentation of high powered laser in air [17]. This was first practically proved by Xin Miao Zhao and his team [8]. It was not until 1990s, that the filamentation in air was observed practically [7], [8].

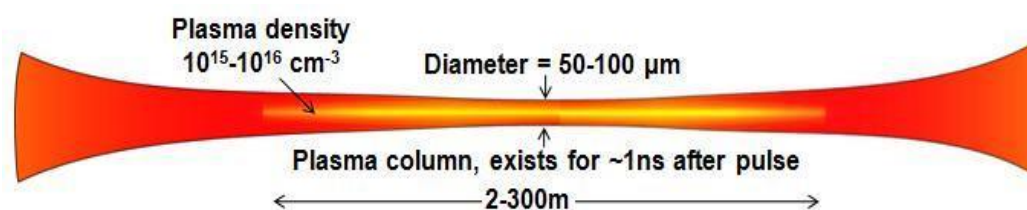


Fig. 1. Image of a filament [16]

Fig.1. depicts a typical image of a filament. It shows a narrow channel of plasma being formed in the center of the laser pulse.

2.2. Properties of ultrashort laser pulse

The initiation of the filamentation process is well understood now. To briefly describe, the process of plasma formation can be described by two effects: the optical Kerr effect and plasma defocusing. In the following, we briefly review some properties that play a role in the process of femtosecond filamentation [17].

2.2.1. Diffraction

The process in which the laser light tends to spread out as a result of passing through different refractive indices is called Diffraction. Laser beam always undergoes the process of diffraction, even while propagating through any medium such as vacuum. The Gaussian optical law states that the width of the beam with a flat spatial phase, increases by $\sqrt{2}$ when the beam propagates over its ‘‘Rayleigh length’’. The Rayleigh length (L_{DF}) is defined as

$$L_{DF} = \frac{\pi n_0 W_0^2}{\lambda_0}$$

Where, W_0 is the width of the beam, λ_0 is the wavelength of the laser in vacuum, n_0 is the refractive index of the medium at λ_0 wavelength [17]. For the laser, we used in the Grigg Hall, the Rayleigh length of the beam with $W_0 = 0.5$ cm at $\lambda_0 = 1.06$ μm in air ($n_0 = 1$, see Appendix I) is $L_{DF} = 74.05$ m. This property is mandatory for the process of filamentation to complete. The Rayleigh length describes that the length (74.05 m) of the laser propagation after which the width of the laser increases by $\sqrt{2}$. That is, in this case, once the laser propagates for 74.05 m, the width of the laser tends to diffract and increase its width from 0.5 cm to 0.71 cm.

2.2.2. Space-time defocusing

It is assumed that the laser pulse has a constant duration in vacuum. Although it might be true but it is not the case all the time. The laser is not made up of one color. It does have blue and red frequencies. The bluer frequencies diffract less than redder frequencies. So, the detector will record a pulse which is longer before it propagated because the pulse spectrum reaching the detector has become narrower. This shows that it can play a significant role in the process of filamentation [17].

2.2.3. Self-focusing

The most important part of the filamentation process is self-focusing. The self-focusing effect of a high-powered laser pulses is due to the optical Kerr effect. The optical Kerr effect describes the intensity-dependent index of refraction [16]:

$$n_1 = n_0 + n_2 I(r, t)$$

Where, n_0 is the linear refractive index, n_2 is the nonlinear refractive index and $I(r, t)$ is the intensity profile of the laser pulse [16]. Typical values of n_2 and n_0 are shown in Appendix I. for self-focusing to occur, the peak power of the laser beam must be higher than critical power [16].

$$P_{cr} \approx \frac{3.77 \lambda_0^2}{8 \pi n_0 n_2}$$

For the laser which was used for this thesis with the wavelength is $1.06 \mu\text{m}$, has the critical power of 0.768 MW (see Appendix I for the values of the calculations).

Once the power of the laser pulse reaches beyond the critical power, the laser beam tends to self-focus as the photons becomes more localized towards the center of the pulse. This central localization lead to plasma at the center of the beam and hence the refractive index of the laser decreases in the center of the beam. This shows that the refractive index in the center of the beam is less and the outer periphery of the laser pulse tries to self-focus and hence it leads to interesting energy dynamics within the pulse [17].

2.2.4. Plasma defocusing

In figure 2.a. the self-focusing of the laser beam is shown. As mentioned before, this phenomenon occurs due to optical Kerr effect. The refractive index of the laser act as a lens, as it is depended on intensity of the laser it makes the beam more focused.

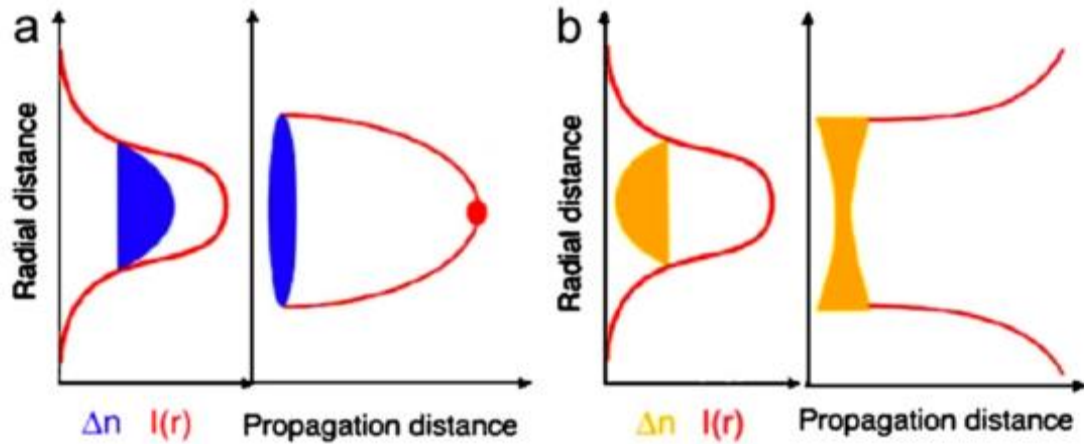


Fig. 2. a. Self-focusing of a beam due to optical Kerr effect. b. Defocusing of the laser beam due to the presence of the plasma [17].

In figure 2.b. the defocusing of the beam is shown. The Δn depicts the change in refractive index and $I(r)$ depicts the intensity profile of the laser beam. The defocusing shown here happens due to the presence of plasma. The reason for defocusing is the same as self-focusing, the change in refractive index. Since the center of the beam has the highest intensity, the ionization of the medium starts at the center. Once the medium is ionized, the plasma is created and the created plasma decreases the local index of the medium, which leads to defocusing [17].

2.2.5. Refocusing cycles

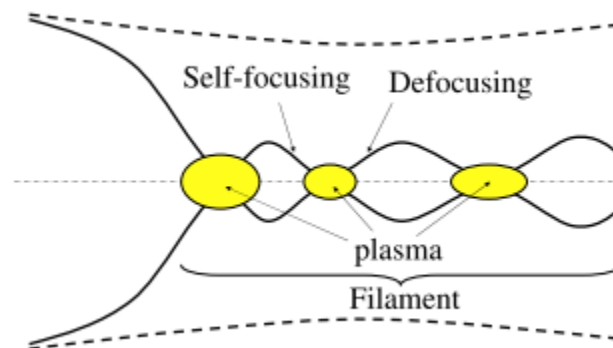


Fig. 3. Schematic representation of the refocusing cycles [17].

The fig. 3. Shows defocusing cycles of the laser beam. It can be easily noticed that the plasma is in the center indicating the intense core of the beam. The solid line indicates the intense core of the beam and the dashed line shows the average diameter of the laser beam. It is evident from the Figure 3 that there are multiple plasma hotspots showing multiphoton ionization (see Appendix III) and the creating multiple filaments. The combination of the plasma makes one filament as shown in the figure [17].

The refocusing cycle, occurs due to the combined action of optical Kerr effect, multiphoton absorption, and ionization (see Appendix III). If the beam tends to defocus, the beam may still self-focus if the average power of the defocused beam is greater than its critical power. The refocusing cycles are very dynamic in nature. This process tends to occur along with the multiphoton ionization and self-focusing cycles [17].

The refocusing cycle can create multiple filaments in air and these filaments will be created if the power of the laser is greater than the critical power of the laser. This filament is created at a distance ‘ Z_f ’ from the source. The filament distance (Z_f) can be calculated using the following formula:

$$Z_f = \frac{0.367 L_{DF}}{\sqrt{\left(\sqrt{\frac{P_{in}}{P_{cr}}} - 0.852\right)^2 - 0.0219}}$$

Where, P_{in} is the input power of the laser (418 mW) and P_{cr} is the critical power of the laser (0.768 MW) and with $L_{DF} = 74.05 \text{ m}$, as calculated before, the filament will be created at 32.41 m.

2.2.6. Filaments in condensed media

All the properties stated above are observed on a reduced scale. The dense transparent dielectrics have nonlinear refractive index larger than gas. Hence, the critical

power of the laser to achieve the self-focus is in the range lesser than the critical power needed in gaseous media due to optical Kerr effect. Normally, the critical power of the laser to self-focus in gaseous media is in the range of GW and in condensed media it is in the range of MW [17].

Filamentation in liquids have been a keen point of interest for many authors such as P. Lallemand and n. Blowmbergen [3]. Water is used normally for experimenting the liquid part of the experiment as, it is easily available and the length of the water channel can be increased easily. For liquids, the shorter the focal length of the laser beam, the smaller the optical breakdown occurs in sufficiently smaller energy threshold. The rest of the condensed media is considered in solids and liquids, where both the state of matter depicts similar characteristics which shows lower energy consumption for self-focusing with compared to air [17].

2.3. Energy dynamics of the filament



Fig. 4. Two regions of a filament [16]

The energy dynamics of a filament is particularly interesting. After the ionization begins, the beam profile is separated into two distinct regions: the inner and the outer ionization region. The inner ionized region has high intensity. The outer region, also called “energy reservoir”, has less intensity but bigger diameter. In a normal filamentation process, the inner region has lower refractive index and photons tends to move out of the center and at the same time, the photons

tend to self-focus and move towards the center. The equilibrium between these two regions makes the filament propagate over long distances via refocusing cycles [17].

There were experiments conducted in which the two regions were separated. This experiment suggests that the outer region truly is the energy reservoir and it is due to this region the filament seems to exist [18], [19] and [20].

2.4. Applications

2.4.1. LIDAR

Light Detection and Ranging (LIDAR), is based on optical scattering phenomenon of the emitted light in atmosphere. During the process of light scattering, a small portion of emitted light is observed at the source, which can be analyzed to understand the result. However, the light which is emitted back to the source is usually weak to detect a presence of a specific substance in the atmosphere. To negate this flaw in the usual LIDAR system, the femtosecond-LIDAR (fs-LIDAR) system can be utilized. The fs-LIDAR is more useful as the femtosecond pulse has a strong white light source, which when pulsed in the atmosphere emits stronger back light to the source. Hence, fs-LIDAR has wide spectral range which can identify trace substances in the atmosphere [21].

In figure 2.a. the self-focusing of the laser beam is shown. As mentioned before, this phenomenon occurs due to optical Kerr effect. The refractive index of the laser act as a lens, as it is depended on intensity of the laser it makes the beam more focused.

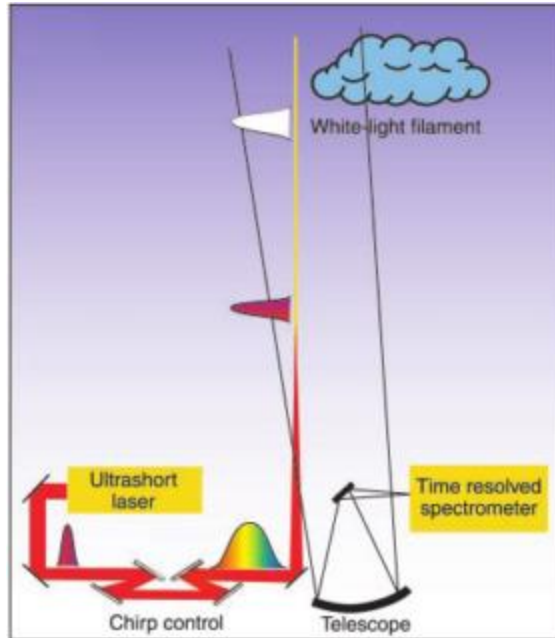


Fig. 5. Schematic diagram of a white-light LIDAR [21]

2.4.2. Laser propulsion

In 2005, Zheng and his team successfully demonstrated the propulsion of a paper airplane using filamentation and without using complicated focusing optics. In the experiment, a filament was produced by the process of filamentation and the plasma channel produced continuously propelled a light paper airplane. It was found that the air serves as the propellant in the plasma channel and detonation wave acts as a propulsive source [22]. Before the femtosecond laser, researchers relied on nanosecond laser. To make the paper airplane propel using nanosecond laser was not possible as it tends to ablate the target material. However, due to advancement in technology, femtosecond filamentation is useful for this application. After this experiment, the plasma channel could be a source for very long distance propulsion [17].

2.4.3. Atmospheric Applications

Atmospheric applications of femtosecond filamentation consist mainly of three types: the LIDAR, Laser Induced Breakdown Spectroscopy (LIBS), rain making and lightning control. LIDAR have already been discussed in Section 2.4.1, Lightning control will be discussed in Section 2.4.4 and LIBS will be discussed in Section 2.4.5. In this Section, we will focus solely on rain making techniques by femtosecond filamentation process.

Condensation is the phenomenon that converts the matter from gaseous state to liquid state. This phenomenon is the backbone of rain making. Although, rain making utilizes two techniques: heavy molecules dispersion and nucleation of germs, to initiate the process of condensation, not always the conditions are right for the rain making. The femtosecond filamentation helps the clouds to supersaturate the atmosphere by adding artificial or natural nucleation of germs. Charges induced by the femtosecond laser filament can serve as nucleation germs to initiate the rain making. Experiments done in fog chamber by Kasparian [21] shows that the water droplets tend to condensate around or near the charges generated by the femtosecond filament. The result shows that there is a strong droplet formation around the laser [17].

2.4.4. Lightning Control

The possibility of guiding a lightning strike and triggering it have been debated over three decades now [23]. The main concern is to protect important sites, such as substations or any high-rise building from lightning strikes. Before the advent of femtosecond laser beam, nanosecond laser was used to initiate lightning control [24]. However, since the femtosecond laser was in use, the nanosecond laser was eliminated as

the femtosecond laser produces ionized plasma channels with plasma density far greater than the required density to create a lightning discharge [21].



Fig. 6. Laser control of high-voltage plasma discharge [21]

In 2002, Rodriguez et al. performed an experiment triggering and guiding of large gap discharges in air via laser filament [25]. The experiment showed that the breakdown voltage is reduced by more than 30% which in turn demonstrates that once the filament is created, the plasma filament channel becomes a part of the discharge path. As seen in Fig. 6, the lightning discharge is erratic in nature initially, but once laser beam passes through the region, the lightning discharge tends to follow the filament. This experiment opens new horizons, such as lightning control over cities, with respect to femtosecond filament-induced triggering of lightning [21].

2.4.5. Laser Induced Breakdown Spectroscopy (LIBS)

The femtosecond filament has the ability to achieve very high intensities of light over long distances for remote sensing and analysis using laser induced breakdown spectroscopy (LIBS) technique. A plasma filament is produced by absorption of the intense laser pulse on the surface. The material which then ablates consists of ions, excited atoms, and excited molecules. This technique could find various applications such as surveying of contaminated wasteland or exhaust from the chimneys of power plant or characterization of industrial scrap materials [17].

CHAPTER 3: LASER-ELECTRICAL FIELD INTERACTION

3.1. Introduction

As mentioned earlier in Section 1.1, the ultrashort and intense laser pulses have been a great interest for the last 40 years [1]. With various applications mentioned in Section 2.4, it was necessary for the researchers to gain in depth knowledge of the topic. There is thus a necessity to understand the role of electric field produced by the laser beam and the role of externally applied electric field on the laser beam for the process of filamentation.

It is known that the laser radiates electric field and its interaction with an external electric field may lead to an outcome that may be useful to one of the applications of the filamentation process. This topic thus needs to be discussed in this thesis. This topic may clarify the role of the externally applied electric field on the laser beam and the process of filamentation.

3.2. Electric field

It is evident that laser produces electric field in its path of propagation and thus the process of filamentation initiates. To support the initiation of filamentation easily, the power of the laser is to be increased. But to increase the laser power, we need to add more energy to the laser system. To opt a different method to increase the laser power, the

external electric field plays a big role. To understand this topic, the electric field of the laser and external system is to be known.

The laser used for the experiments had an average power of 418 mW with a beam radius of 5 mm. Calculating the electric field of the laser setup,

$$E = \sqrt{\frac{2 I}{c \epsilon_0}}$$

Where, 'E' is the electric field of the laser beam; 'I' is the laser intensity; 'c' is the speed of light and ' ϵ_0 ' is the vacuum permittivity. Also,

$$I = \frac{P}{A}$$

Where, 'P' is the power of the laser and 'A' is the area of the laser beam.

Substituting the values in the electric field formula:

$$E = \sqrt{\frac{2 P}{c \epsilon_0 A}}$$

In the above formula, the power of the laser 'P' is 418 mW, the speed of light 'c' is 3×10^8 m/sec, the vacuum permittivity ' ϵ_0 ' is 8.85×10^{-12} F/m and the area of the laser beam is 0.0157 m^2 . Substituting all the values in the formula, we find out that the electric field produced by the laser system is 141.61 V/m.

In the experiment setup, there is four different electrode geometries that produce different electric field to the system. These setups are discussed in detail in Section 4.2. The main goal of the experiment is to record the power of the laser after it passes through the electrode setup and compare it to the power of the laser before it passed through the setup.

Considering the complete laser path through the electrode setup, the area of the laser that is influenced by the electric field is different than calculated before. Here, the area of the laser is calculated by considering it as a Gaussian cylinder compared to just a circle as in the previous calculation. Considering the laser as a cylinder, the length of the laser that passes through the electrode varies in all four geometries. In electrode setup T1, the length of the laser is 3 cm; in T2, the length of the laser is 4 cm; in T3, the length of the laser is 5 cm; and in T4, the length of the laser is 8 cm.

Calculating the area of the laser in all four geometries T1, T2, T3 and T4: $2.04 \times 10^{-3} \text{ m}^2$, 0.011 m^2 , 0.021 m^2 and 0.048 m^2 respectively. Hence, the electric field of the laser inside the electrode setup T1, T2, T3 and T4 is 392.87 V/m, 169.18 V/m, 122.44 V/m, and 80.99 V/m respectively.

As mentioned before, the effect of external electric field is to be considered on the laser and its own electric field. One way to consider its effect is to compare both the electric fields of the laser and the one which is applied externally. Two high voltage sources that produce the external electric field are 10 kV AC and 30 kV DC respectively. The formula that calculates the electric field is:

$$E = \frac{V}{L}$$

Where, 'E' is the electric field, 'V' is the applied voltage, and 'L' is the length between the two plates of the electrode. The length 'L' of the electrode varies in all four geometries T1, T2, T3 and T4: 3 cm, 4 cm, 5 cm, and 8 cm respectively. Hence, the AC electric field of the laser inside the electrode setup T1, T2, T3 and T4 is 333.33 kV/m, 250 kV/m, 200 kV/m, and 125 kV/m respectively and the DC electric field of the laser inside

the electrode setup T1, T2, T3 and T4 is 1000 kV/m, 750 kV/m, 600 kV/m, and 375 kV/m respectively.

Comparing the electric fields of the laser system and the AC and DC external system:

Table 1: Comparing the electric field values of the laser system and externally applied electric field

Electrode setup	Laser electric field	AC electric field	DC electric field
T1	392.87 V/m	333.33 kV/m	1000 kV/m
T2	169.18 V/m	250.00 kV/m	750 kV/m
T3	122.44 V/m	200.00 kV/m	600 kV/m
T4	80.99 V/m	125.00 kV/m	375 kV/m

From Table 1, it is easily noticed that the electric field of the laser is lower than that of the external electric field. The external electric field is in order of kV/m and the electric field of the laser system is in terms of the V/m. Comparing them shows that the applied electric field is about 1000 times stronger than the laser electric field and may not provide interaction between the two systems of laser and external electric field. To understand the interaction between the two systems is by the process of ionization. The process of ionization occurs by the process of Avalanche breakdown. This process occurs when there is a high voltage applied to a pair of electrode plates and air in and around the electrode plates get ionized and form ions. These ions, depending on their size and charge, tend to go from one plate to another. Later, this effect ionizes more air in the area and tend to create a least resistive path between the electrode plate and tend to create a breakdown and this

happens in an instant and hence it is called the Avalanche effect. This breakdown happens in form of a glow discharge and is generally termed plasma.

There are different ways to create discharge: electric arc discharge, vacuum arc discharge, glow discharge etc. But mainly this phenomenon explained takes place in all the different ways to generate plasma with some minor changes in the equipment. For example, in glow discharge, the medium that is ionized is not air, it is an inert gas. Also, in electric arc discharge, the electric field is applied to a pair of electrode that produce electric arc with high temperature and high current. These are various methods to create plasma discharge and there is electric field associated with it and hence it could play a vital role in the interaction between the electric field of the laser and electric field of the external power source.

CHAPTER 4: LASER POWER MEASUREMENT

4.1. Introduction

Although the topic of filament creation and the investigation of the filament has been studied by many researchers since its inception, the topic of the interaction between the laser and an externally provided electric field has not yet been investigated. In this thesis, this topic is examined by recording the power of the laser before and after the interaction of the laser with electric field and low temperature plasma.

There are four electrode designs tested in the thesis for electric field and plasma generation. The four types of electrodes have different geometrical features that vary spatially and tend to produce electric field and plasma differently. The experiment setup has been described in detail in Section 4.2.

The research goal is to see whether there is any change in the power of the laser when the laser interacts with electric field and low temperature plasma. The laser power is recorded and analyzed as it plays an important role in initiating the filamentation process.

4.2. Experiment Setup

The experiment was conducted in Grigg Hall room 108, where the Tsunami and RegA femtosecond laser is housed. Tsunami ultrafast oscillator in combination with RegA laser amplifier that creates the femtosecond laser in the infrared regime. The average power of the laser is 418 mW with its wavelength $1.06 \mu\text{m}$ and frequency 1 PHz. The laser was

focused via the help of mirrors and was made to pass through the electric field and/or plasma of the different electrodes. Figure 7 depicts the laser setup.

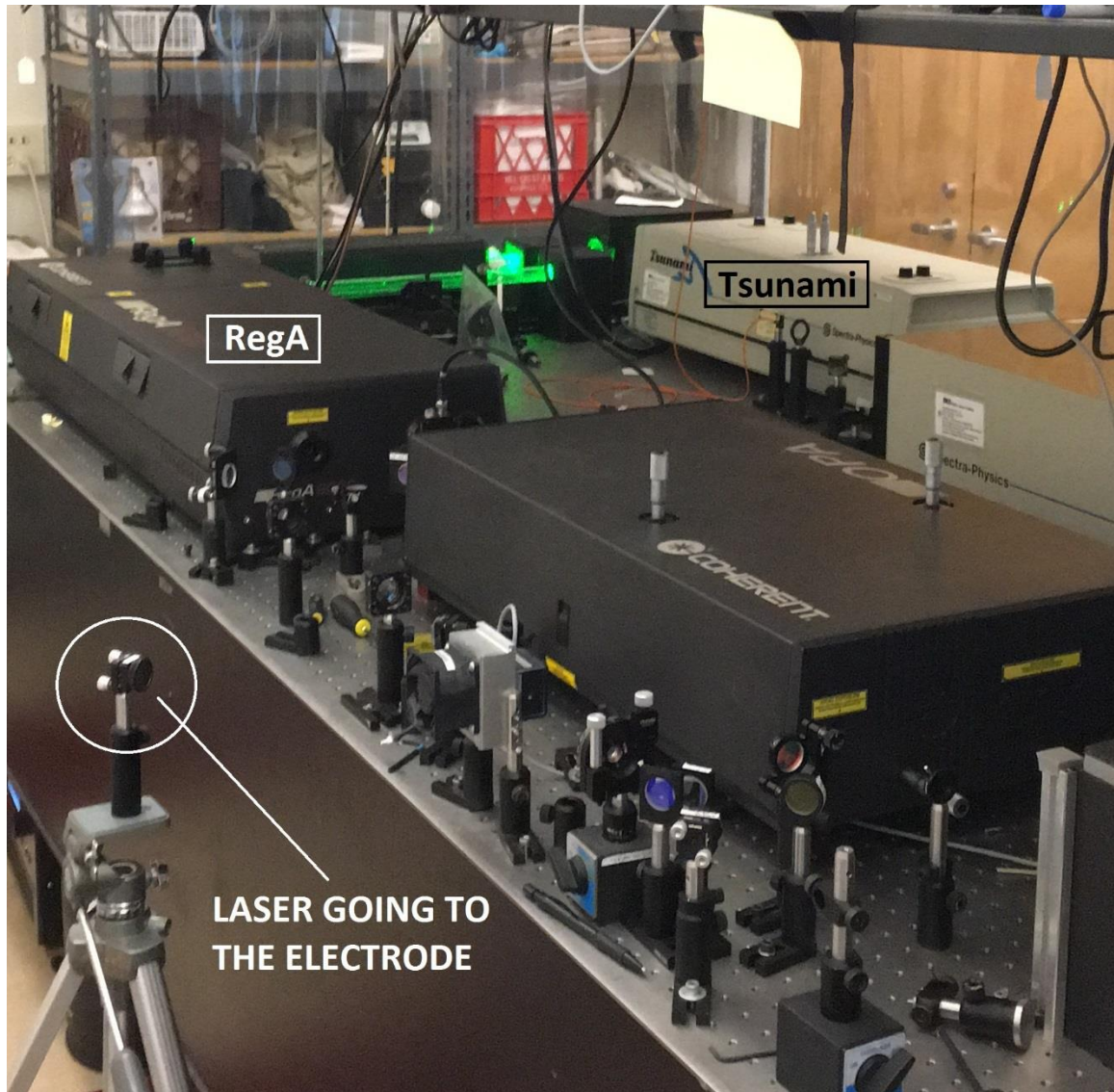


Fig. 7. Laser setup at Grigg 108. This setup shows the reflective mirrors from which the laser is shun towards the electrode setup.

The above figure depicts the laser setup in Grigg 108. The laser setup consists of two laser setups of Tsunami and RegA. The laser beam which initiates from the Tsunami oscillator passes to RegA laser amplifier which produces the femtosecond laser which is passed towards the reflective mirrors and then towards the electrode setup. This setup is

depicted schematically in Figure 8, which shows the full laser setup with the laser path going towards the electrode setup.

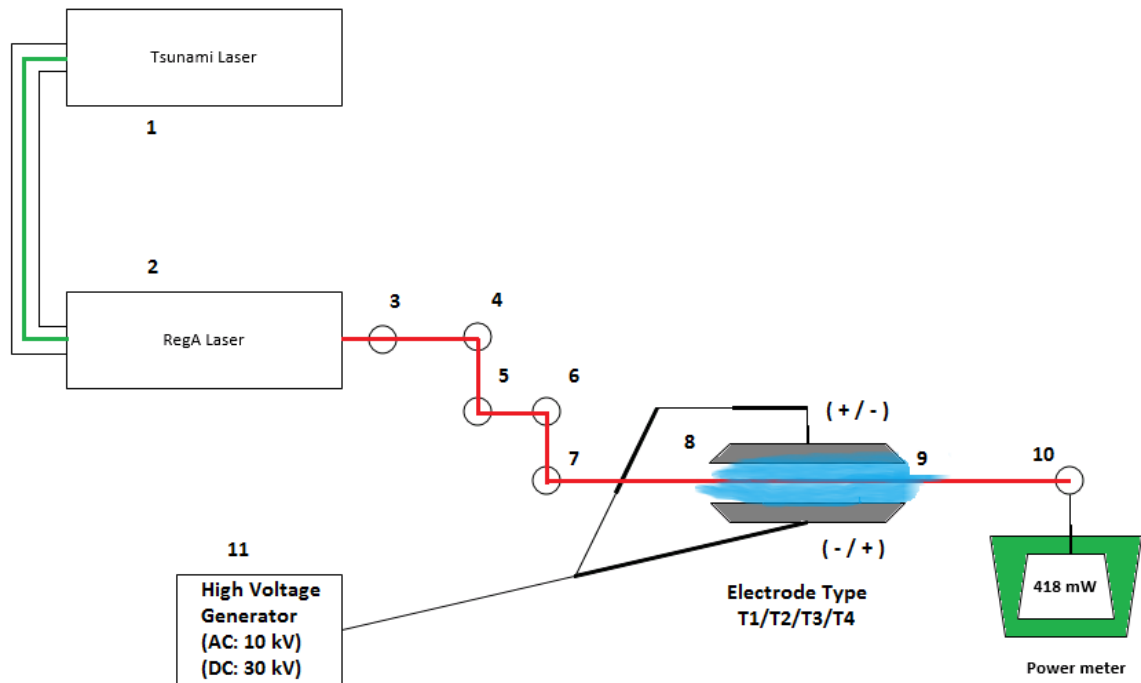


Fig. 8. Schematic diagram of the laser setup in the Grigg Hall with the electrode in the path of the laser

Figure 8 depicts the schematic diagram of the laser system along with the electrode geometry. Equipment number 1 and 2 are the Tsunami oscillator and the RegA is a power amplifier of the laser system. These two systems in total make up the laser. Equipment number 3-7 are reflective mirrors for adjusting the path of the laser and is used to make the laser pass through the electrode system (equipment 8). The electrode system is either T1, T2, T3 or T4. This electrode system produces the electric field and/or plasma (Point 9) with the help of high voltage generator (equipment 11). This generator is either 30 kV DC Matsusada EQ series generator or a 10 kV AC Trek Model 624 A series-001 generator.

Once the laser is fired from the laser system, the laser passes through the plasma and/or electric field (point 9) towards the Coherent LabMaster Ultima power meter (equipment 10). This meter has an accuracy of +/- 3% and is mounted on a tripod stand parallel to the electrode setup. The power meter is used to measure the power of the reading before the presence of electric field and/or plasma and after the interaction of the laser with electric field and/or plasma.

In Figure 8, as mentioned before, the equipment 8 depicts the electrode system. For the thesis, there are four electrode setups used during experimentation.

4.2.1. Parallel plate electrode (T1)

The most basic type of electrode geometry is the parallel plate electrode (T1). As the name suggests, T1 consists of two parallel plates which is given a high voltage DC or AC supply. This helps to create electric field and/or low temperature plasma discharge. Figure 14 depicts the electric field present between two electric fields. The strength of the electric field lines (orange color) is calculated by Formula $E = \frac{V}{L}$. This electrode system, shown in Figure 15, produces the electric field in order of 333.33 kV/m with AC source and 1000 kV/m in DC source. The goal of the experiment is to measure the laser beam power when it is made to shine through the electric field in electrode setup T1.

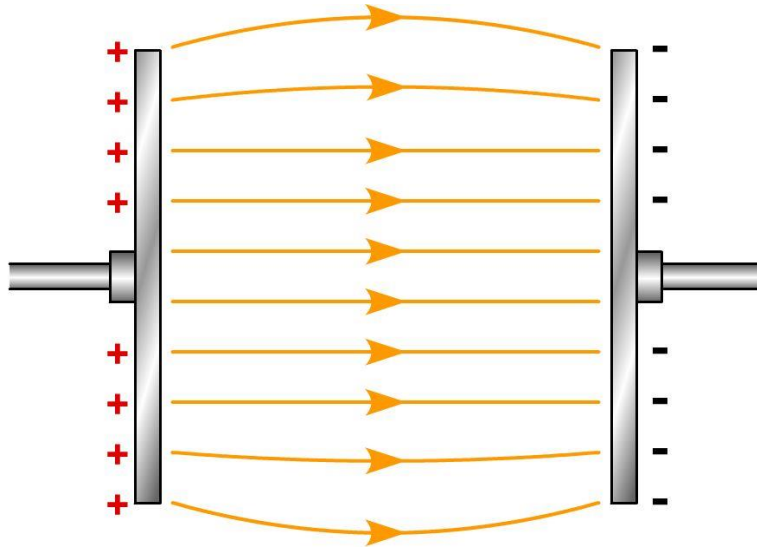


Fig. 9. Schematic diagram of the electric field through T1
(<http://iamtechnical.com/sites/default/files/electric-fields.jpg>)

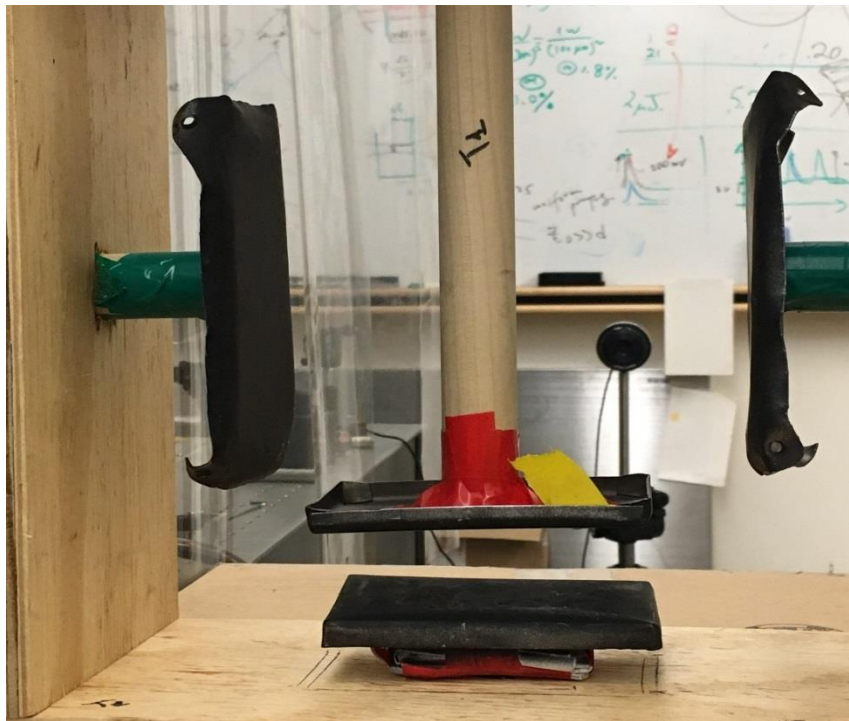


Fig. 10. Parallel plate electrode (T1)

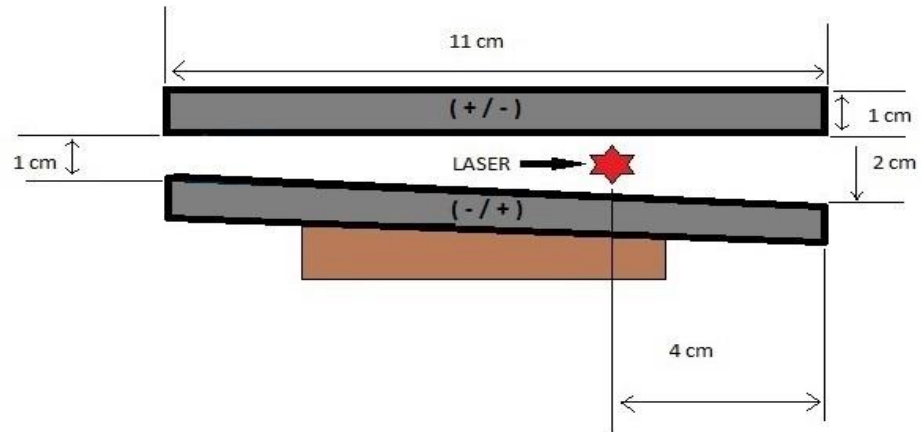


Fig. 11. Schematic of T1 electrode and the path of laser during the experiment.

Figure 11 depicts the place of the laser when it passes through the electric field produced by the T1 electrode. The laser power is measured by the power meter before and after the interaction of laser with the electric field.

4.2.2. 'V' shaped electrode (T2)

'V' shaped electrodes (T2) are different electrode design which has the steel and aluminum plates bent in 'V' shaped. As seen in Figure 12, the T2 electrode consists of 'V' bent steel and aluminum plates.

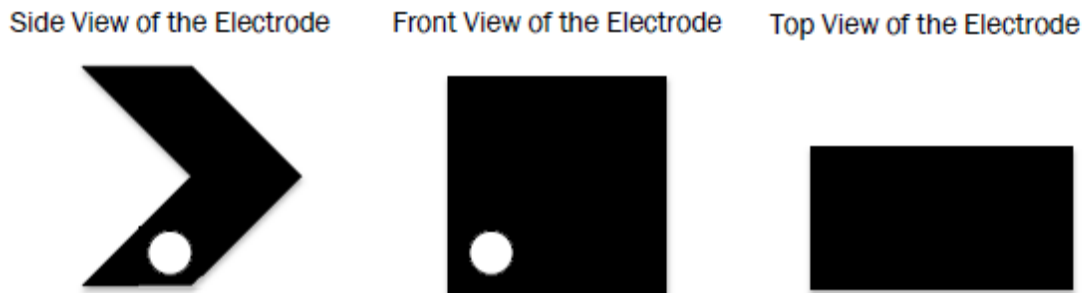


Fig. 12. T2 electrode geometry

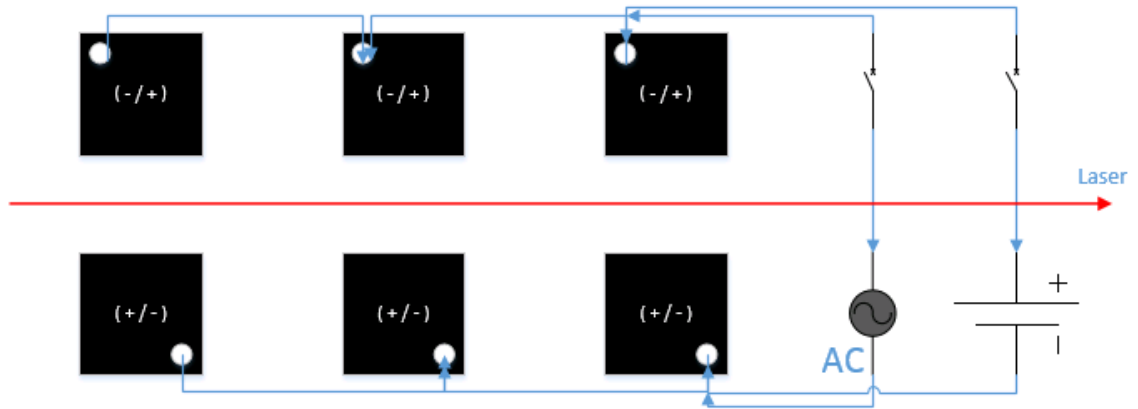


Fig. 13. T2 electrode connection and path of the laser



Fig. 14. 'V' shaped electrode system

4.2.3. Needle electrodes (T3)

Needle electrodes (T3) is the third type of the electrode. This design is different from T1 from two aspects. One, the electrode here is a needle electrode and is more pointed

Figure 13 shows the schematic diagram of the T2 electrode.

Figure 14 shows the 'V' shaped electrode system used during the experiment mounted on wooden stands. This electrode setup produces the electric field in order of 250 kV/m with AC source and 750 kV/m in DC source.

than the T1 electrode. This configuration leads to stronger electric field and easier plasma discharge due to its pointed structure. Two, the needle electrodes are separated spatially, which could provide continuous electric field in the path of the laser.

Figure 15 shows the schematic diagram of the laser path and the needle electrode placement. This would allow the laser to interact with stronger to electric field and/or plasma discharge. Figure 15, shows the T3 electrode with its needle like electrode, made up of screws, pointing outwards from the base.

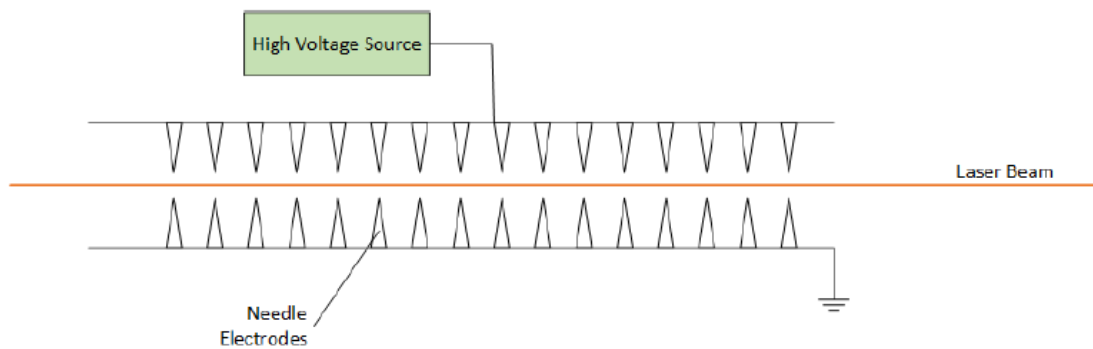


Fig. 15. Schematic diagram of T3 electrode and the path of laser.

This electrode setup produces the electric field in order of 200 kV/m with AC source and 600 kV/m in DC source.

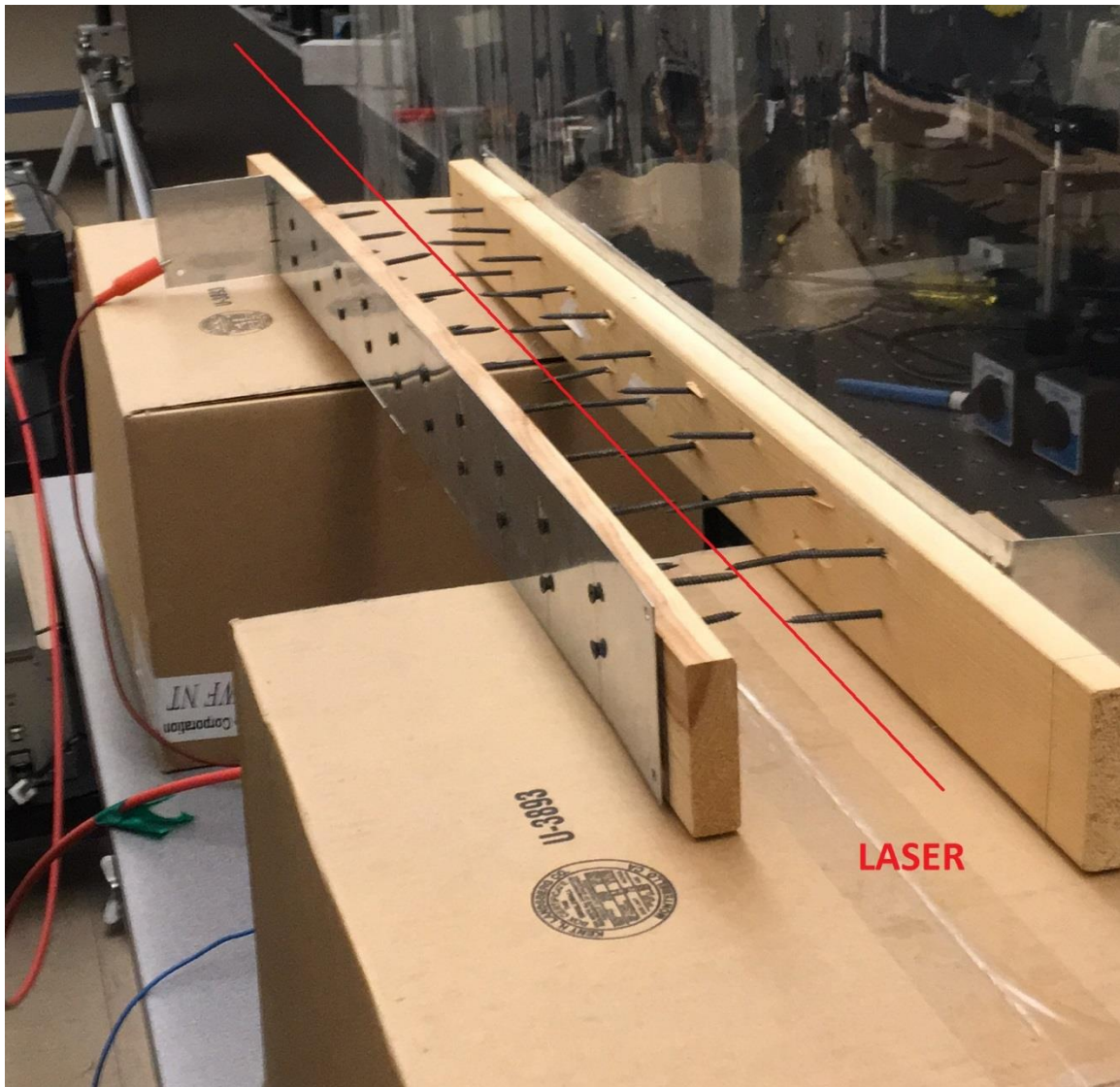


Fig. 16. T3 electrode and the virtual path of the laser.

4.2.4. Double helix shaped electrode (T4)

The double helix shaped electrode (T4) is the fourth and the last type of electrode design to be tested in the design. This shape has the needle electrodes placed in double helix shape. This would provide pseudo AC electric field effect which is more focused and spatially separated, when AC/DC high voltage supply is given to the test electrode.

The effect of the electric field produced by 10 kV AC and 21 kV DC was observed when the laser was shunned through the electrode. Figure 17 shows the T4 from outside

and Figure 18 and 19 depicts the inside geometry of the T4 electrode. The electric field produced by this test electrode is 125 kV/m in AC and 375 kV/m in DC.



Fig. 17. Double helix electrode (T4)

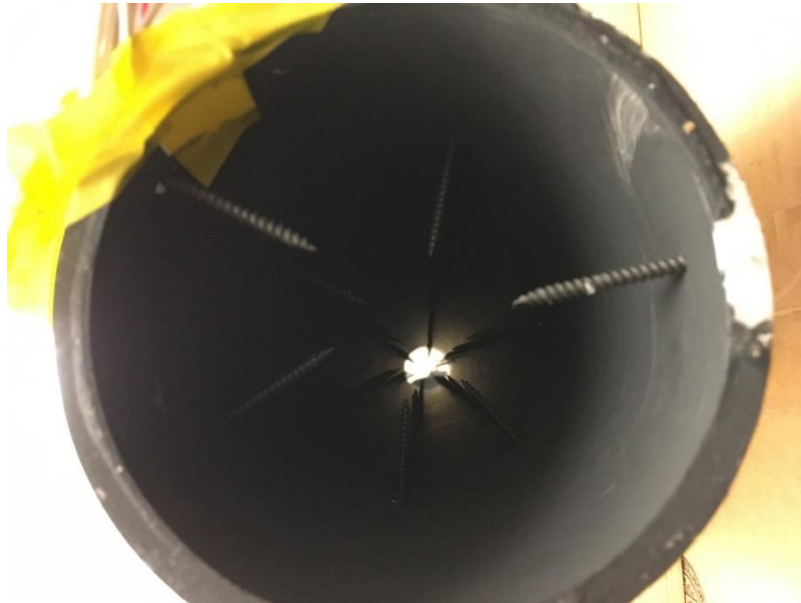


Fig. 18. Inside geometry of T4 electrode.

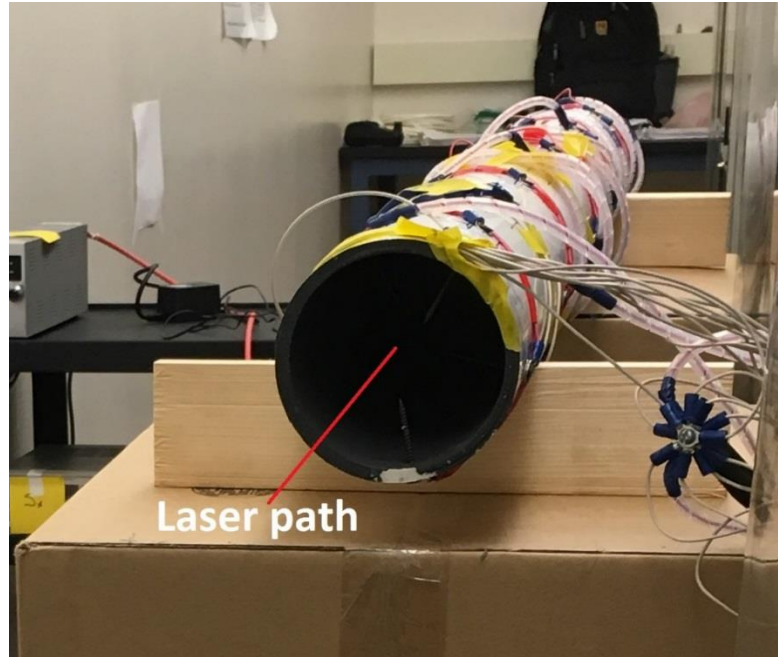


Fig. 19. Inside geometry of T4 electrode with laser beam path.

4.3. Results

The DC and AC sources energizes the four electrode setups one at a time in experiment 1 and experiment 2 respectively. The laser is made to shine through each electrode setup in each experiment where the power of the laser is measured before and after the laser passes through electrode setup. In Experiment 2, the experiment where AC source is used to create the electric field, the frequency of the supply is varied to see the effect of different frequencies of the electric field on the laser beam. The section below presents the results obtained during the experiments performed in the laser lab.

The average power of the laser recorded before the presence of the electric field and/or plasma discharge is 418 mW. As mentioned before, there are two experiments conducted on T1 with DC and AC high voltage source. The limit to the high voltage DC source was found out to be 21 kV as it reached its breakdown current limit. So, the maximum voltage that was applied to the electrode systems was 21 kV.

In the result tables, the power (P) depicts the power of the laser after its interaction of laser with the electric field in the electrode setup. The change in power (ΔP) describes the effect of the electric field and the plasma discharge on the laser beam. The frequency represents the change in frequency in the AC field using a frequency modulator. Recall that the power meter has an accuracy of $\pm 3\%$, which means the error bar of the graphs plotted for the power of the laser, 418 mW, ranges from the minimum of 405 mW to 430 mW (shown as a blue box in the graph).

4.3.1. Parallel plate electrode (T1)

Experiment 1: Applying up to 21,000 V DC

Table 2: Experimental result for T1 electrode DC supply

V (kV)	P (mW)	ΔP
0	418	0
10	415	-3
15	410	-8
21	406	-12

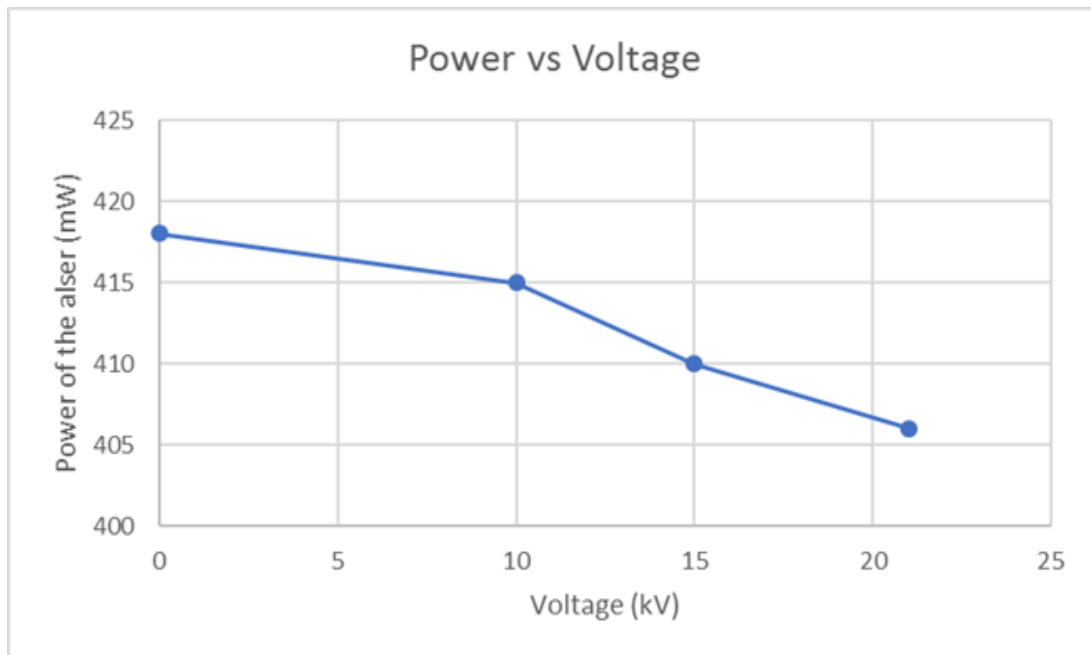


Fig. 20. Influence of DC Electric field on T1 electrode system

Experiment 2: Applying 10,000 V AC with varied frequency

Table 3: Experimental result for T1 electrode AC supply

F (kHz)	P (mW)	ΔP
0.1	422	+4
0.5	420	+2
1	418	0
1.5	413	-5
2	410	-8
2.5	402	-16
3.5	398	-20

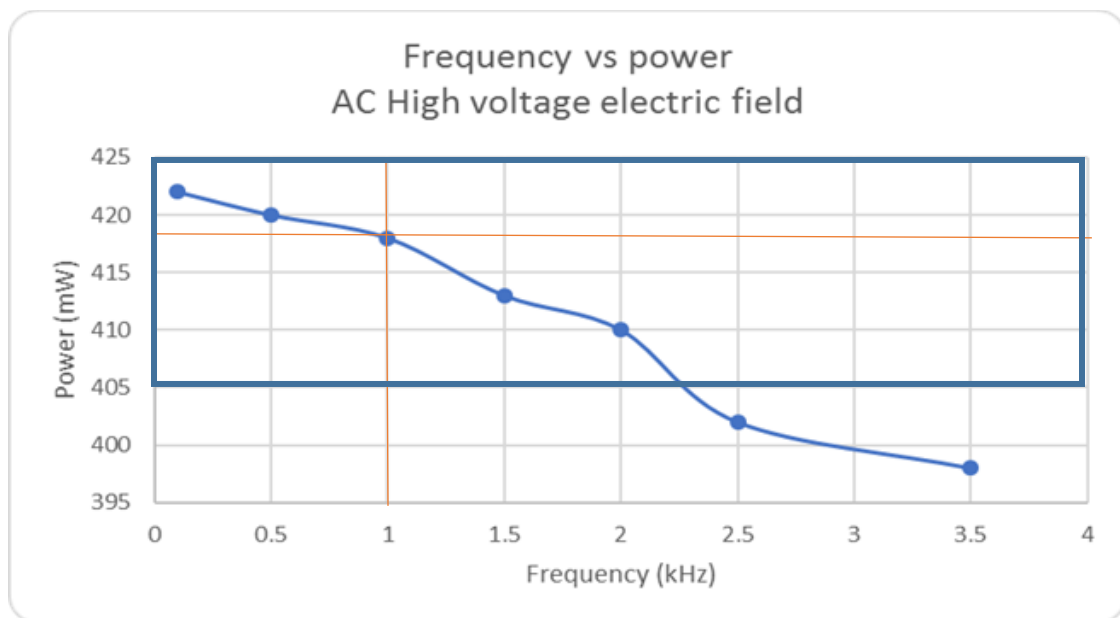


Fig. 21. Influence of AC Electric field on T1 electrode system

4.3.2. 'V' shaped electrode (T2)

Experiment 1: Applying up to 21,000 V DC

Table 4: Experimental result for T2 electrode DC supply

V (kV)	P (mW)	ΔP
0	418	0
10	417	-1
15	419	+1
21	416	-2

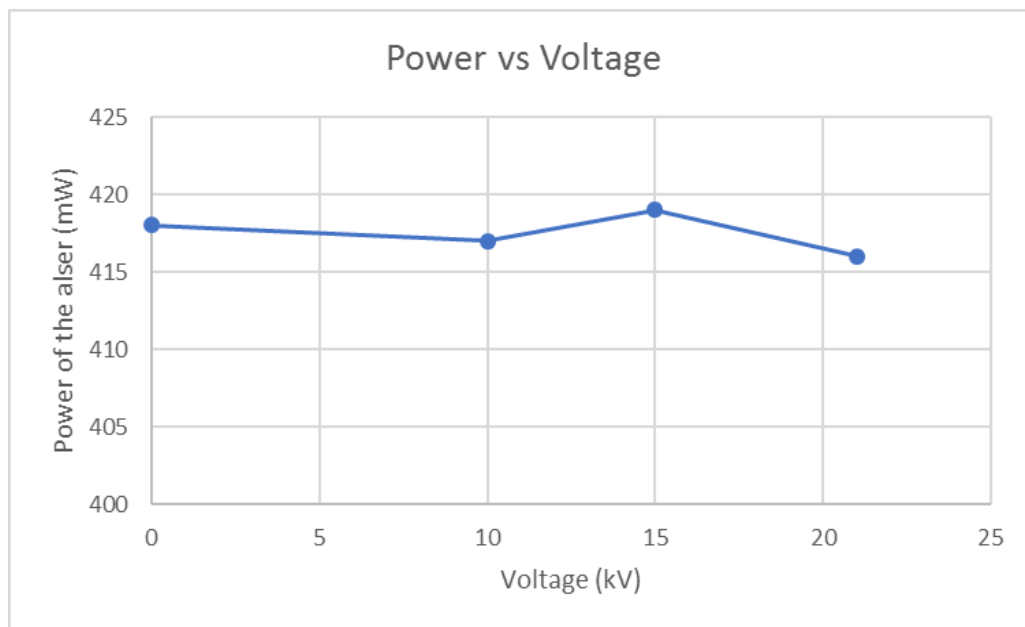


Fig. 22. Influence of DC Electric field on T2 electrode system

Experiment 2: Applying 10,000 V AC with varied frequency

Table 5: Experimental result for T2 electrode AC supply

F (kHz)	P (mW)	ΔP
0.1	421	+3
0.5	419	+1
1	418	0
1.5	415	-3
2	408	-10
2.5	404	-14
3.5	399	-19

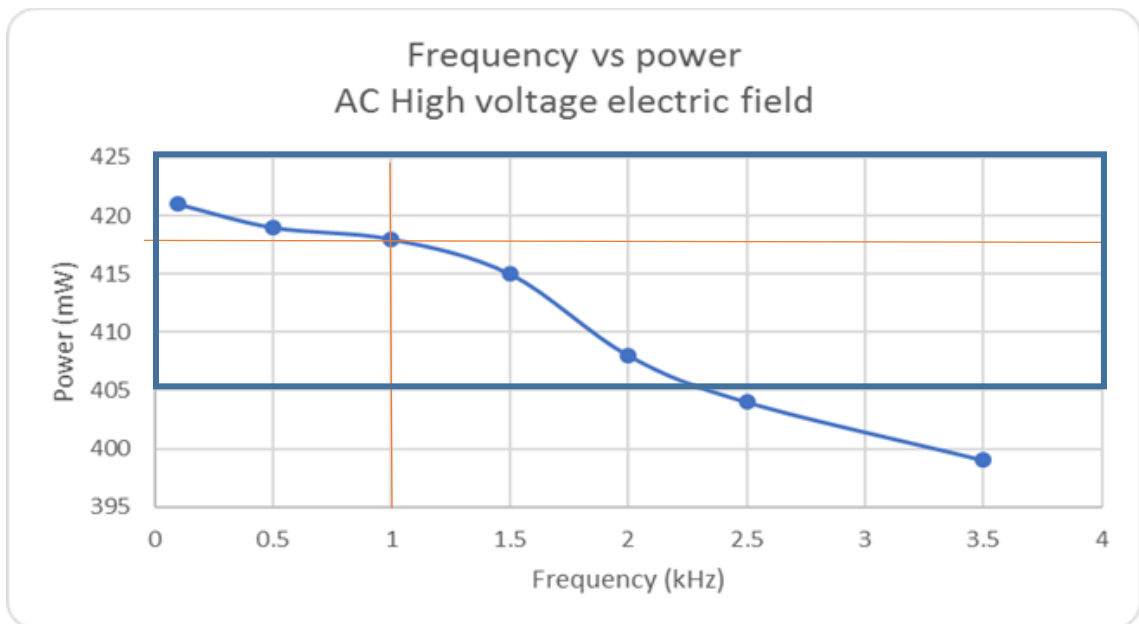


Fig. 23. Influence of AC Electric field on T2 electrode system

4.3.3. Parallel plate electrode separated spatially (T3)

Experiment 1: Applying up to 21,000 V DC

Table 6: Experimental result for T3 electrode DC supply

V (kV)	P (mW)	ΔP
0	418	0
10	412	-6
15	409	-9
21	404	-14

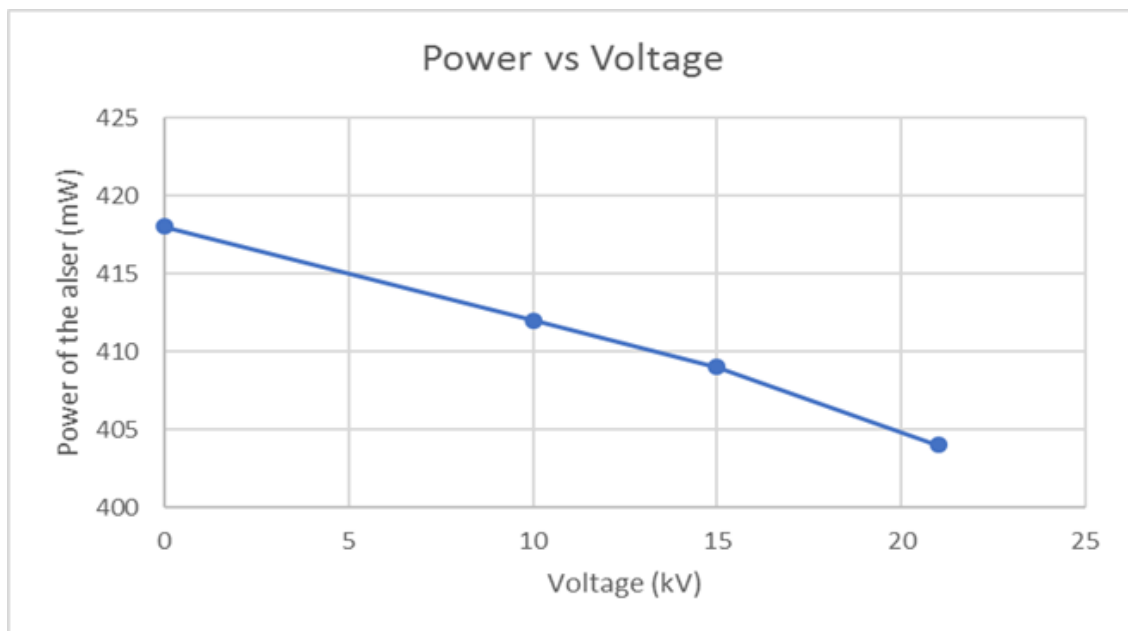


Fig. 24. Influence of DC Electric field on T3 electrode system

Experiment 2: Applying 10,000 V AC with varied frequency

Table 7: Experimental result for T3 electrode AC supply

F (kHz)	P (mW)	ΔP
0.1	422	+4
0.5	420	+2
1	418	0
1.5	414	-4
2	411	-7
2.5	408	-10
3.5	400	-18

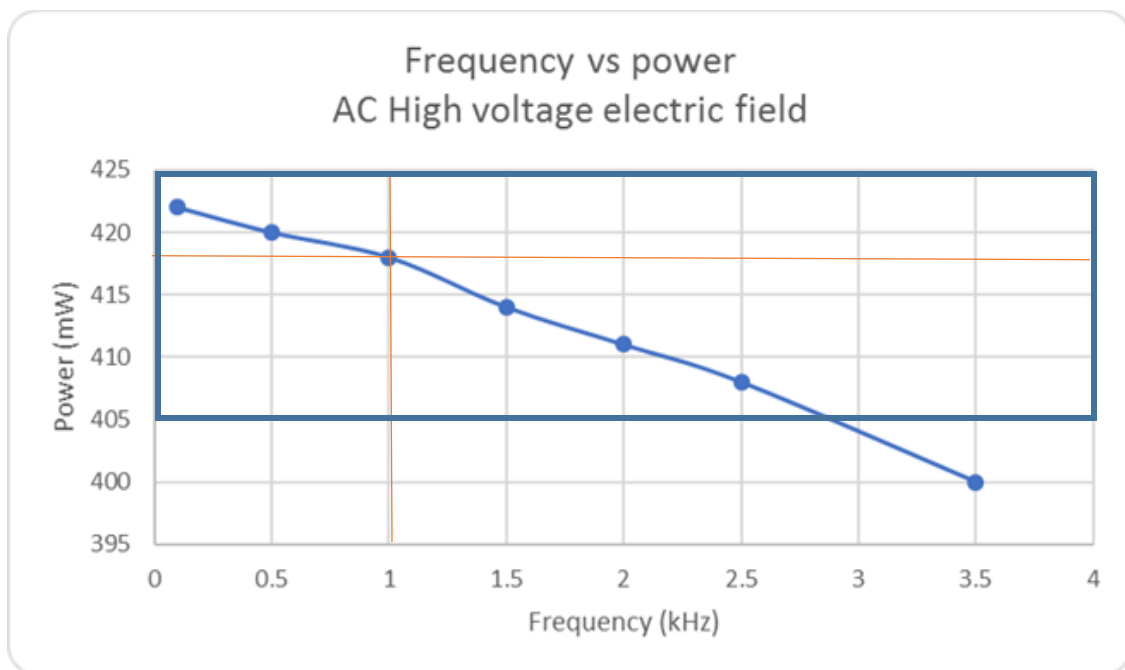


Fig. 25. Influence of AC Electric field on T3 electrode system

4.3.4. Double helix shaped electrode (T4)

Experiment 1: Applying up to 21,000 V DC

Table 8: Experimental result for T4 electrode DC supply

V (kV)	P (mW)	ΔP
0	418	0
10	419	+1
15	421	+3
21	423	+5

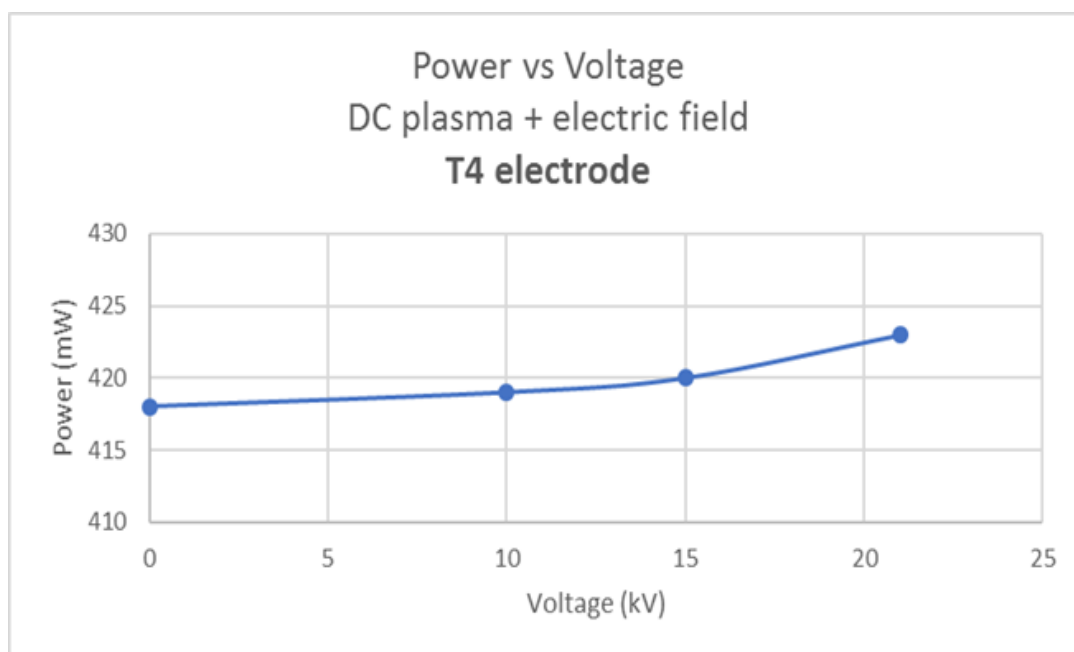


Fig. 26. Influence of DC Electric field on T4 electrode system

Experiment 2: Applying 10,000 V AC with varied frequency

Table 9: Experimental result for T4 electrode AC supply

F (kHz)	P (mW)	ΔP
0.1	424	+6
0.5	421	+3
1	418	0
1.5	415	-3
2	412	-6
2.5	411	-7
3.5	402	-16

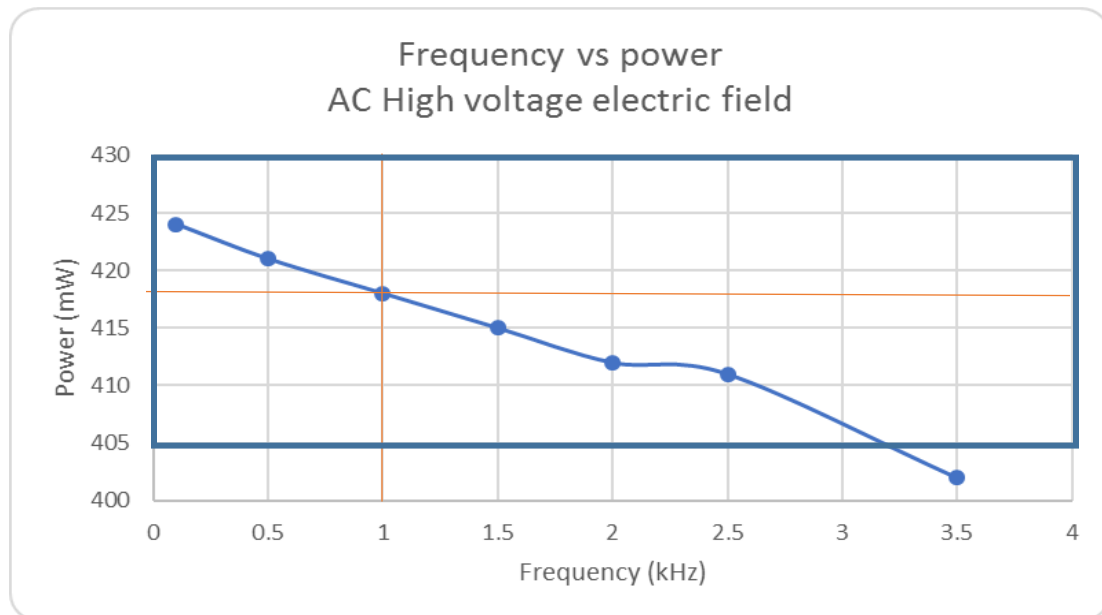


Fig. 27. Influence of AC Electric field on T4 electrode system

CHAPTER 5: PROBABLE CONCLUSIONS AND DISCUSSIONS

In all the experiments, it has been observed that the externally applied electric field influences the power of the laser. There is a trend to be noticed in the results that were observed. In the experiment 1, the trend shows decrease in power in T1 and T3 electrode system and a constant power trend in electrode systems T2 and T4. In experiment 2, the trend shows that there is an increase in the power of the laser with decrease in frequency of the high voltage supply and there is a decrease in power of the laser with increase in frequency of the high voltage supply.

The probable conclusion from the trends are the following: In experiment 1, the electrode setup T2 and T4 have no significant interaction with the DC field, and hence there is no change in the power of the laser before and after its interaction with the electric field. For electrode setup T1 and T3, the power reduces and this can be explained by comparing the electric field of the laser to the high voltage supply. As mentioned before, the electric field of laser in T1 and T3 are 392.87 V/m and 122.44 V/m respectively, whereas the electric field of the high voltage supply in T1 and T3 for experiment 1 are 1000 kV/m and 600 kV/m respectively. Comparing both the values, it is seen that the electric field of the high voltage supply is greater than the electric field by more than 1000 time. This would mean that the stronger electric might take up energy from the laser and

may lead to losses in the laser propagation. Hence, the power of the laser decreases in electrode T1 and T3.

In experiment 2, all the electrodes show similar characteristics, that is there is an increase in the power of the laser with decrease in frequency of the high voltage supply and there is a decrease in power of the laser with increase in frequency of the high voltage supply. This is a strange behavior considering different results from the previous experiment. The process of producing electric field in air leads to ionization of air, that is, there are ions being produced due to high voltage supply and that the ions that are present between the electrodes that play a role in the behavior of the laser that shines through the ions. It is a possibility that since the electric field of the high voltage supply is stronger, there are more ions that are produced in the path of the laser and hence the ions block the path of the laser and its power decreases. To understand the increase of the laser power after its interaction with the ions, we need to understand the working of a laser (see Appendix II). As Appendix II suggest, when ionized gas is given charge, one of the ion emits light and with continuous energy, there is a cascade of light emission and that leads to laser light. The same phenomenon works here in the electrode system too. There is ionized air between the electrode with many free ions, which when is made to interact with laser, tends to get converted to photons, hence increasing the power of the laser.

There were times when low temperature plasma was produced and the laser was made to shine through it, which showed the same results as depicted before. The explanation for increment in power remains same for power decrement there is a possibility of plasma blocking the path of the laser due to shutter effect. Even when the laser did not

pass the plasma discharge, the power of the laser decreased, may be due to the partial shutter effect of high voltage plasma discharge [32].

5.1. Summary of the thesis

The main intent of the thesis was to find out if the externally applied electric field or ionization can lower the power of the laser needed to start the process of filamentation. But over the course of this research, the finding shown in the results section suggest some phenomenon partially understood by the author.

To summarize, the power of the laser can be increased or decreased by making it interact with external electric field. This thesis proves empirically, that there is a relation between the frequency of the electric field and the power of the laser beam. The results suggest that the power of the laser beam is inversely proportional to the frequency of the electric field.

5.2. Future work

This thesis asks more research questions that it answers, but it opens an interesting set of findings which can lead to many different applications. Future work may lead to conducting the experiments in vacuum to know whether the increment or decrement of the laser power is due to high voltage electric field and plasma discharge or due to the presence of air. Along with this, the effect of electric field and ionized species on the laser beam is to be understood.

REFERENCES

- [1] G. A. Askar'yan, "Effects of the gradient of a strong electromagnetic beam on electrons and atoms," *Top. Appl. Phys. Top. Appl. Phys.*, vol. 114, pp. 269–271, 2009.
- [2] M. Hercher, "Reprints of Papers from the Past," in *Self-focusing: Past and Present: Fundamentals and Prospects*, R. W. Boyd, S. G. Lukishova, and Y. R. Shen, Eds. New York, NY: Springer New York, 2009, pp. 267–294.
- [3] P. Lallemand and N. Bloembergen, "Self-Focusing of Laser Beams and Stimulated Raman Gain in Liquids," *Phys. Rev. Lett.*, vol. 15, no. 26, pp. 1010–1012, Dec. 1965.
- [4] E. Garmire, R. Y. Chiao, and C. H. Townes, "Dynamics and Characteristics of the Self-Trapping of Intense Light Beams," *Phys. Rev. Lett.*, vol. 16, no. 9, pp. 347–349, Feb. 1966.
- [5] J. H. Marburger, "Self-focusing: Theory," *Progr. in Quant. Electron.*, vol. 4, pp. 35–110, 1975.
- [6] L. S. Chin, W. Liu, F. Théberge, Q. Luo, A. S. Hosseini, P. V. Kandidov, G. O. Kosareva, N. Aközbek, A. Becker, and H. Schroeder, "Some Fundamental Concepts of Femtosecond Laser Filamentation," in *Progress in Ultrafast Intense Laser Science III*, Berlin, Heidelberg: Springer Berlin Heidelberg, 2008, pp. 243–264.
- [7] A. Braun, G. Korn, X. Liu, D. Du, J. Squier, and G. Mourou, "Self-channeling of high-peak-power femtosecond laser pulses in air," *Opt. Lett.*, vol. 20, no. 1, pp. 73–75, 1995.

- [8] Xin Miao Zhao, J.-C. Diels, Cai Yi Wang, and J. M. Elizondo, “Femtosecond ultraviolet laser pulse induced lightning discharges in gases,” *IEEE J. Quantum Electron.*, vol. 31, no. 3, pp. 599–612, Mar. 1995.
- [9] B. La Fontaine, F. Vidal, Z. Jiang, C. Y. Chien, D. Comtois, A. Desparois, T. W. Johnston, J.-C. Kieffer, H. Pépin, and H. P. Mercure, “Filamentation of ultrashort pulse laser beams resulting from their propagation over long distances in air,” *Phys. Plasmas*, vol. 6, no. 5, p. 1615, 1999.
- [10] P. Rairoux, H. Schillinger, S. Niedermeier, M. Rodriguez, F. Ronneberger, R. Sauerbrey, B. Stein, D. Waite, C. Wedekind, H. Wille, L. Wöste, and C. Ziener, “Remote sensing of the atmosphere using ultrashort laser pulses,” *Appl. Phys. B*, vol. 71, no. 4, pp. 573–580, 2000.
- [11] G. Méjean, J. Kasparian, J. Yu, S. Frey, E. Salmon, and J.-P. Wolf, “Remote detection and identification of biological aerosols using a femtosecond terawatt lidar system,” *Appl. Phys. B*, vol. 78, no. 5, pp. 535–537, 2004.
- [12] K. Stelmaszczyk, P. Rohwetter, G. Méjean, J. Yu, E. Salmon, J. Kasparian, R. Ackermann, J.-P. Wolf, and L. Wöste, “Long-distance remote laser-induced breakdown spectroscopy using filamentation in air,” *Appl. Phys. Lett.*, vol. 85, no. 18, p. 3977, 2004.
- [13] D. A. Cremers and L. J. Radziemski, “Remote LIBS Measurements,” in *Handbook of Laser-Induced Breakdown Spectroscopy*, John Wiley & Sons Ltd, 2013, pp. 257–287.
- [14] T. A. Labutin, V. N. Lednev, A. A. Ilyin, and A. M. Popov, “Femtosecond laser-induced breakdown spectroscopy,” *J. Anal. At. Spectrom.*, vol. 31, no. 1, pp. 90–

- 118, 2016.
- [15] H. Wille, M. Rodríguez, J. Kasparian, D. Mondelain, J. Yu, A. Mysyrowicz, R. Sauerbrey, J.-P. Wolf, and L. Woeste, “Teramobile: a mobile femtosecond-terawatt laser and detection system,” *Eur. Phys. J. Appl. Phys.*, vol. 20, no. 3, pp. 183–190, 2002.
- [16] D. Nicholson, “Laser Pulse Filamentation Some Physics Behind Self - Focusing,” 2011. [Online]. Available: <http://large.stanford.edu/courses/2011/ph240/nicholson1/>.
- [17] A. Couairon and A. Mysyrowicz, “Femtosecond filamentation in transparent media,” *Phys. Rep.*, vol. 441, no. 2–4, pp. 47–189, 2007.
- [18] A. Dubietis, E. Kucinskas, G. Tamosauskas, E. Gaizauskas, M. A. Porras, and P. Di Trapani, “Self-reconstruction of light filaments,” *Opt. Lett.*, vol. 29, no. 24, pp. 2893–2895, 2004.
- [19] M. Kolesik and J. V. Moloney, “Self-healing femtosecond light filaments,” *Opt. Lett.*, vol. 29, no. 6, pp. 590–592, 2004.
- [20] F. Courvoisier, V. Boutou, J. Kasparian, E. Salmon, G. Méjean, J. Yu, and J. P. Wolf, “Ultraintense light filaments transmitted through clouds,” *Appl. Phys. Lett.*, vol. 83, no. 2, pp. 213–215, 2003.
- [21] J. Kasparian, M. Rodriguez, G. Méjean, J. Yu, E. Salmon, H. Wille, R. Bourayou, S. Frey, Y.-B. André, A. Mysyrowicz, R. Sauerbrey, J.-P. Wolf, and L. Wöste, “White-Light Filaments for Atmospheric Analysis,” *Science (80-.)*, vol. 301, no. 5629, pp. 61–64, 2003.
- [22] Z.-Y. Zheng, J. Zhang, Z.-Q. Hao, Z. Zhang, M. Chen, X. Lu, Z.-H. Wang, and Z.-

- Y. Wei, "Paper airplane propelled by laser plasma channels generated by femtosecond laser pulses in air.," *Opt. Express*, vol. 13, no. 26, pp. 10616–10621, 2005.
- [23] D. W. Koopman and T. D. Wilkerson, "Channeling of an ionizing electrical streamer by a laser beam," *J. Appl. Phys.*, vol. 42, no. 5, pp. 1883–1886, 1971.
- [24] M. Miki, T. Shindo, and Y. Aihara, "Mechanisms of guiding ability of laser-produced plasmas on pulsed discharges," *J. Phys. D. Appl. Phys.*, vol. 29, no. 7, pp. 1984–1996, 1999.
- [25] M. Rodriguez, R. Sauerbrey, H. Wille, L. Wöste, T. Fujii, Y.-B. André, A. Mysyrowicz, L. Klingbeil, K. Rethmeier, W. Kalkner, J. Kasparian, E. Salmon, J. Yu, and J.-P. Wolf, "Triggering and guiding megavolt discharges by use of laser-induced ionized filaments," *Opt. Lett.*, vol. 27, no. 9, pp. 772–774, 2002.
- [26] T. A. Physics, "Episode 405: Preparation for electric fields topic," *Gatsby Technical Education Projects (GTEP)*, 2011. [Online]. Available: http://tap.iop.org/fields/electrical/405/page_46857.html.
- [27] F. Physics, "Electric field simulation." [Online]. Available: <http://www.flashphysics.org/electricField.html>.
- [28] T. A. Physics, "Episode 406: Fields field lines and equipotentials," *Gatsby Technical Education Projects (GTEP)*, 2011. [Online]. Available: http://tap.iop.org/fields/electrical/406/page_46863.html.
- [29] T. A. Physics, "Episode 409: Uniform electric fields," *Gatsby Technical Education Projects (GTEP)*, 2011. [Online]. Available: http://tap.iop.org/fields/electrical/409/page_46894.html.

- [30] Emspak Jesse, “States of Matter: Plasma,” 2016. [Online]. Available: <http://www.livescience.com/54652-plasma.html>.
- [31] P. International, “Perspectives on Plasmas,” 2004. [Online]. Available: <http://www.plasmas.org/basics.htm>.
- [32] E. Yablonovitch, “The Physics of Laser-Plasma Interaction in Gaseous Targets,” in *Laser Interaction and Related Plasma Phenomena*, Boston, MA: Springer US, 1977, pp. 367–386.

APPENDIX I: List of refractive indices

List of refractive indices for common media [16]

<i>Material</i>	n_0 (dimensionless)	n_2 (cm ² /W)
<i>Air</i>	1.003 \approx 1	5.0 x 10 ⁻¹⁹
<i>Vacuum</i>	1	1.0 x 10 ⁻³⁴
<i>Water</i>	1.33	>4.1 x 10 ⁻¹⁶
<i>Fused silica</i>	1.47	3.2 x 10 ⁻¹⁶
<i>BK-7</i>	1.52	3.4 x 10 ⁻¹⁹

Table 10: List of refractive indices for common media

APPENDIX II: Working of a gas laser

The working of a laser is simple. To make a laser, energy is to be given to a collection of electrons to make them excited and emit light. Once one of the electron is excited to a level where it emits light, it will stimulate the other excited electrons to emit the light along with it, creating a cascade effect of illumination. This, when enclosed between a fully reflective mirror and a semi-reflective mirror enclosure, tends to bounce the light more and energizes the photons even more. This will continue to do so until the atoms are excited. In general, photons tend to have same phase, polarization and orientation and hence the cascade effects lead to more emission of photons. This when emitted from a small opening from the semi-reflective mirror, produces laser.

APPENDIX III: Ionization process

Multi-Photon Absorption: The process where multiple photons are absorbed together at once is called a Multiphoton absorption. In a semiconductor or an insulator, the electrons get absorbed only when the photon energy is at least as large as bandgap energy. At high optical intensities, this bandgap can be overpassed by simultaneous absorption or lower-energy photons, whose total photon energies surpasses the bandgap energy. These types of processes are called multi-photon ionization. An example of Multi-photon absorption is laser-induced damage in transparent media. More detailed explanation could be found on: https://www.rp-photonics.com/multiphoton_absorption.html.

Ionization: ionization process can be divided into two major categories: photoionization. Furthermore, the photoionization can be subdivided into three categories: single photoionization, multiphoton ionization, and tunnel ionization. The difference between the three subdivisions are the number of ions being ionized to produce the effect. For single photoionization, the energy required to ionize a single photon is needed to create the ionization process. For multiphoton ionization, multiple ions are ionized together to create the ionization process. Tunnel ionization occurs when the electric field of the laser is so strong that it pulls off an electron from the atom. On the other hand, Collisional ionization is for longer pulses such as a nanosecond pulsed laser. During this, the electrons quiver in the electric field and when the energy applied to it is high enough, the electron is easily detached from the atom. More detailed explanation could be sound on: <https://physics.stackexchange.com/questions/277427/can-a-powerful-enough-laser-ionize-nitrogen-in-the-air-along-the-lasers-beam>.